THE JOURNAL OF BIOLOGICAL CHEMISTRY
Vol. 279, No. 25, Issue of June 18, pp. 26220–26226, 2004

Printed in U.S.A.

Jingzhaotoxin-III, a Novel Spider Toxin Inhibiting Activation of Voltage-gated Sodium Channel in Rat Cardiac Myocytes*

Received for publication, February 8, 2004, and in revised form, April 13, 2004
Published, JBC Papers in Press, April 14, 2004, DOI 10.1074/jbc.M401387200

Yucheng Xiao, Jianzhou Tang, Yuejun Yang, Meichi Wang, Weijun Hu, Jinyun Xie, Xiongzhi Zeng, and Songping Liang‡

From the College of Life Sciences, Hunan Normal University, Changsha, Hunan 410081, People's Republic of China

We have isolated a cardiotoxin, denoted jingzhaotoxin-III (JZTX-III), from the venom of the Chinese spider *Chilobrachys jingzhao*. The toxin contains 36 residues stabilized by three intracellular disulfide bridges (I-IV, II-V, and III-VI), assigned by a chemical strategy of partial reduction and sequence analysis. Cloned and sequenced using 3′-rapid amplification of cDNA ends and 5′-rapid amplification of cDNA ends, the full-length cDNA encoded a 63-residue precursor of JZTX-III. Different from other spider peptides, it contains an uncommon endoproteolytic site (-*X*-Ser-) anterior to mature protein and the intervening regions of 5 residues, which is the smallest in spider toxin cDNAs identified to date. Under whole cell recording, JZTX-III showed no effects on voltage-gated sodium channels (VGSCs) or calcium channels in dorsal root ganglion neurons, whereas it significantly inhibited tetrodotoxin-resistant VGSCs with an IC_{50} value of 0.38 μM in rat cardiac myocytes. Different from scorpion β-toxins, it caused a 10-mV depolarizing shift in the channel activation threshold. The binding site for JZTX-III on VGSCs is further suggested to be site 4 with a simple competitive assay, which at 10 μM eliminated the slowing currents induced by *Buthus martensi* Karsch I (BMK-I, scorpion α-like toxin) completely. JZTX-III shows higher selectivity for VGSC isoforms than other spider toxins affecting VGSCs, and the toxin hopefully represents an important ligand for discriminating cardiac VGSC subtype.

Voltage-gated sodium channels (VGSCs)[1] are trans-membrane proteins distributed widely in the most excitable tissue. Similar to the *shaker* potassium channel (1), the three-dimensional structure of sodium channel is a bell-shaped molecule determined by helium-cooled cryo-electron microscopy and single particle image analysis (2). In terms of tetrodotoxin (TTX), they can be classified into TTX-sensitive (TTX-S) and TTX-resistant (TTX-R) types. More recently, from mammals including human, more than 10 mammalian ($Na_v1.1$–$Na_v1.9$ and Na_vx) subtypes have been identified, cloned, functionally expressed, and characterized (3). Most of them can express in dorsal root ganglion (DRG) neurons, except for $Na_v1.4$ in skeletal muscles and $Na_v1.5$ in cardiac myocytes (4). These subtypes have been highly conserved during evolution (5, 6). With more than 75% sequence identity among one another, they exhibit relatively similar pharmacological properties in different expression systems. However, it is the divergent residues among the sequences of these VGSC isoforms that determine their response to distinct ligands. For instance, after tyrosine 371 is substituted by serine in rNav1.6 and rNav1.3 (wild types), which are TTX-S phenotypes, the mutants become resistant to TTX (7, 8).

As the major contributors to the initiation and propagation of action potentials, VGSCs become the main targets attacked by many spider toxins. With specific pharmacological properties and higher affinity with VGSCs, spider peptides have attracted the interests of many scientists. Until now, more than 30 sodium channel toxins have been purified and well characterized from venoms of various species. NMR and homology modeling techniques indicate that, irrespective of the different composition of amino acids, most of them adopt a typical inhibitor cystine knot (ICK) fold distinct from the α/β scaffold emerging in scorpion toxins (9, 10). Most residues in their primary structure are believed to support the peptide framework, whereas only a few charged residues situated at the loop domains of ICK motifs are critical to interact with sodium channels. Recently, scorpion toxin determinants demonstrate that some conserved aromatic residues (Phe, Tyr, and Trp) also play an important role in modifying the sodium channel activities (11). Spider toxins exhibit limited sequence identity in the sodium channel toxins from other origins, such as marine animals, scorpions, and snakes, revealing that there is a perspective for searching for new valuable ligands to dissect variant VGSCs. Furthermore, spider toxins have been shown to lead to new insecticides and pharmaceuticals. On the functional α subunit of VGSCs, more than six sites (sites 1–6) have been disclosed to bind certain ligands (12). Spider toxins mainly interact with three of them, corresponding to blocking channel pore (site 1, hainantoxin-IV (HNTX-IV) and Huwentoxin-IV (HWTX-IV)), slowing channel inactivation (site 3, μ-agatoxins and δ-atracotoxins), and inhibiting channel activation (site 4, Magi 5 and ProTx I–II), respectively (13–18). Most of them are found to have high affinity with the subtypes of VGSCs localizing on sensory neurons, but a few affect the cardiac isoform.

In this study, we report the isolation, cDNA sequence clone, and functional characterization of a novel cardiotoxin from the spider *Chilobrachys jingzhao*, which was identified as a new species recently (19). The crude venom is lethal to mice with an intrapertoneal LD_{50} of 4.4 mg/kg. The spider toxin, denoted

* This work was supported by the National Science Foundation of China under Contract 30170193. The costs of publication of this article were defrayed in part by the payment of page charges. This article must therefore be hereby marked "*advertisement*" in accordance with 18 U.S.C. Section 1734 solely to indicate this fact.

‡ To whom correspondence should be addressed. Tel.: 86-731-8872556; Fax: 86-731-8861304; E-mail: liangsp@hunnu.edu.cn.

[1] The abbreviations used are: VGSC, voltage-gated sodium channel; VGPC, voltage-gated potassium channel; VGCC, voltage-gated calcium channel; TTX, tetrodotoxin; TTX-R, TTX-resistant; TTX-S, TTX-sensitive; JZTX-III, jingzhaotoxin-III; HNTX-IV, hainantoxin-IV; HWTX-IV, Huwentoxin; DRG, dorsal root ganglion; RACE, rapid amplification of cDNA ends; ICK, inhibitor cystine knot; BMK-I, *B. martensi* Karsch I; RP-HPLC, reverse phase-high pressure liquid chromatography; MALDI-TOF, matrix-assisted laser desorption/ionization-time of flight; TCEP, Tris (2-carboxyethyl) phosphine.

jingzhaotoxin-III (JZTX-III), is composed of 36 amino acid residues including 6 cysteines cross-linked in a pattern of I-IV, II-V, and III-VI. The toxin shows no effect on voltage-gated potassium channels (K_v1.1–1.3) expressed in *Xenopus laevis* oocytes or VGSCs and voltage-gated calcium channels (VGCCs) distributed in DRG neurons. However, it can selectively inhibit activation of TTX-R VGSCs in cardiac myocytes followed by shifting activated voltage in a depolarizing direction. We further assume that JZTX-III binds to site 4 on sodium channel proteins, which is formed by amino acid residues in the extracellular linker between domain II-S3 and domain II-S4.

MATERIALS AND METHODS

Toxin Purification and Sequencing—The venom from female *C. jingzhao* spiders was collected as described earlier (16). Lyophilized venom (1 mg in 0.2 ml in distilled water) was applied to a Vydac C18 analytical reverse-phase (RP) HPLC column (218TP54, 4.6 × 250 mm) and eluted at a flow rate of 1 ml/min by a linear gradient of 0–40% of buffer B (acetonitrile containing 0.1% v/v trifluoroacetic acid) over 50 min after an equilibrium period of 3 min with buffer A (distilled water containing 0.1% v/v trifluoroacetic acid). The fraction containing JZTX-III was purified further on the same RP-HPLC column by a slower linear gradient of 30–35% buffer B over 20 min. Once purified to >99% homogeneity assessed by RP-HPLC and mass spectrometry, the peptide sample was lyophilized and stored at −20 °C until use. The molecular mass was determined by MALDI-TOF mass spectrometry on a Voyager-DE™ STR Biospectrometry™ work station. The entire amino acid sequence was obtained from a single sequencing run on an Applied Biosystems/PerkinElmer Life Sciences Procise 491-A protein sequencer.

Identification of JZTX-III cDNA—The characterization of JZTX-III cDNA was performed using 3′- and 5′-RACE methods described previously (20). First, according to the manufacturer's instructions, the total RNA was extracted from 0.1 g of fresh venom glands of female spiders using the TRIzol reagent kit. 5 μg of RNA was taken to convert mRNA into cDNA using the Superscript II reverse transcriptase with an universal oligo(dT)-containing adapter primer (5′-GGCCACGCGTCGACTAGTAC $(dT)_{17}$-3′). The cDNA was then used as a template for PCR amplification in 3′-RACE. A degenerate primer 1 (5′-GG(A/T/C/G)CA(G/A)TT(T/C)TGGTGGAA(A/G)TG(T/C)-3′) was designed corresponding to the N-terminal residues (^{5}GQFWWKC^{11}) of mature JZTX-III. The cDNA of mature toxin was amplified using primer 1 and an abridged universal adapter primer containing an additional HindIII restriction site (5′-CGAAGCTTGGCCACGCGTCGACTAGTAC-3′). Second, based on the partial cDNA sequence of JZTX-III determined by 3′-RACE, the antisense primers were designed and synthesized for 5′-RACE as follows: the gene-specific primer 2 (5′-GCAGGCATACCCTTTGCAGCA-3′) corresponding to the C-terminal residues (^{18}CCKGYAC^{24}). With the strategy described by the RACE kit supplier, the 5′-end cDNA of JZTX-III was amplified using its gene-specific primer 2. Amplified products in both 3′- and 5′-RACE were precipitated and cloned into the pGEM-T easy vector for sequencing. DNA sequencing was performed by Bioasia Inc. Nucleic acid sequences were analyzed using the software DNAclub (by Xiongfong Chen) (www.imtech.res.in/pub/nsa/dnaclub/dos/) and DNAman (by Nynnon Biosoft) (www.Lynnon.com).

Assignment of the Disulfide Bonds of JZTX-III—To determine the disulfide connections of JZTX-III, partial reduction by Tris (2-carboxyethyl) phosphine (TCEP) at low pH was employed (16, 21). 0.1 mg of JZTX-III, dissolved in 10 μl of 0.1 M citrate buffer (pH 3) containing 6 M guanidine-HCl, was partially reduced by adding 10 μl of 0.1 M TCEP at 40 °C for 8 min at pH 3. The intermediates were isolated by RP-HPLC, and their masses were measured by MALDI-TOF mass spectrometry. Appropriate intermediates containing free thiols were dried and then alkylated by adding 100 μl of 0.5 M iodoacetamide (pH 8.3). The alkylated peptide was desalted by RP-HPLC and then submitted to an Applied Biosystems 491 protein sequencer.

Preparation of Cardiac Myocytes—Single ventricular cardiomyocytes were enzymatically dissociated from adult rats by a previously described method (22) with minor modifications. Briefly, Sprague-Dawley rats (about 250 g) of either sex were killed by decapitation without anesthetization, and the heart was rapidly removed and rinsed in ice-cold Tyrode's solution containing (in mM): 143.0 NaCl, 5.4 KCl, 0.3 NaH_2PO4, 0.5 $MgCl_2$, 10.0 glucose, 5.0 HEPES, 1.8 $CaCl_2$ at pH 7.2. Then the heart was mounted on a Langendorff apparatus for retrograde perfusion via the aorta with non-recirculating Ca^{2+}-free Tyrode's solution bubbled at 37 °C by 95% O_2 and 5% CO_2. After 10 min, perfusate was switched to a Ca^{2+}-free Tyrode's solution supplemented with 0.3% collagenase IA and 0.7% bovine serum albumin, and the hearts were perfused in a recirculated mode for 5 min. After the enzymatic solution was replaced by KB buffer containing (in mM): 70.0 L-glutanic, 25.0 KCl, 20.0 taurine, 10.0 KH_2PO_4, 3 $MgCl_2$, 0.5 EGTA, 10.0 glucose, 10.0 HEPES at pH 7.4, the partially digested hearts were cut, minced, and gently triturated with a pipette in the KB buffer at 37 °C for 10 min. The single cells were obtained after undigested tissues filtered through 200-μm nylon mesh. All cells were used within 8 h of isolation.

Electrophysiological Studies—Whole cell cardiac sodium currents were recorded from rod-shaped cells with clear cross-striations at room temperature (20–25 °C). Recording pipettes (2–3-μm diameter) were made from borosilicate glass capillary tubing, and their resistances were 1–2 megaohms when filled with internal solution containing (in mM): 135.0 CsF, 10.0 NaCl, 5.0 HEPES at pH 7.0. External bath composition was (in mM): 30 NaCl, 5 CsCl, 25 D-glucose, 1 $MgCl_2$, 1.8 $CaCl_2$, 5 HEPES, 20 triethanolamine-chlorine, 70 tetramethylammonium chloride at pH 7.4. Ionic currents were filtered at 10 kHz and sampled at 3 kHz on EPC-9 patch clamp amplifier (HEKA Electronics). Linear capacitive and leakage currents were subtracted by using a P/4 protocol. Experimental data were acquired and analyzed by the program pulse+pulsefit8.0 (HEKA Electronics). The needed concentrations of toxin dissolved in external solution were applied onto the surface of experimental cells by low pressure injection with a microinjector (IM-5B, Narishige).

Data Analysis—Data analysis was performed using Pulsefit (HEKA Electronics) and Sigmaplot (Sigma). All data are presented as means ± S.E., and n is the number of independent experiments. The fitted curves of concentration-dependent inhibition were obtained by using the following form of the Boltzmann equation: $\text{Inhibition}\% = 100/[1+\exp(C - IC_{50})/k]$, in which IC_{50} is the concentration of toxin at half-maximal inhibition, k is the slope factor, and C is the toxin concentration.

RESULTS

Purification and Sequence Analysis of JZTX-III—A typical RP-HPLC chromatogram of the female spider venom was shown in Fig. 1*A*, in which more than 20 fractions eluted were monitored at 280 nm. The fraction with the retention time of 38 min, containing JZTX-III, was further purified by a repeated RP-HPLC (Fig. 1*B*). Two purifications yielded about 0.05 mg of JZTX-III/mg of crude venom with a purity over 99%. Its molecular mass was determined to be 3919.4 Da by MALDI-TOF mass spectrometry. The complete amino acid sequence of the toxin was obtained by Edman degradation and found to contain 36 residues including 6 cysteines (see Fig. 4*A*). After being reduced by dithiothreitol and then alkylated with iodoacetamide, the molecular mass of JZTX-III increased 348 Da (58 Da × 6), implying that all 6 cysteines were involved in forming three disulfide bridges. Since the primary structure had a mass of 3919.52 Da, consistent with the measured mass, the C-terminal residue could not be amidated. JZTX-III is a basic peptide sharing less than 50% sequence identity with any know peptides, although its 6 cysteines were highly conserved at corresponding positions in many toxins, such as HWTX-IV, ProTx-I, and ProTx-II (16, 17).

Determination of the Disulfide Bridges in JZTX-III—Because vicinal cysteines (^{18}CC^{19}) emerge in the primary structure of JZTX-III, a chemical strategy composed of partial reduction and sequence analysis was introduced instead of a traditional enzymatic method. As shown in Fig. 2, four main peaks were obtained from the RP-HPLC separation of the partial reduced mixture of JZTX-III by TCEP. MALDI-TOF mass spectrometry analysis points out that the two intermediates yielded were resolved to contain one or two disulfide bridges in peak II and I, respectively, whereas peaks *R* and *N* represent completely reduced peptide and intact peptide, respectively. Peaks I–II were collected and alkylated rapidly with iodoacetamide followed by further purification using analytical RP-HPLC. Molecular mass determination and sequencing indicated that the free thiols of these two peptides had been alkylated.

In Fig. 3*A*, Pth-CM-Cys signals were observed at the 4th and 19th cycles in the sequencing chromatograms of alkylated peak

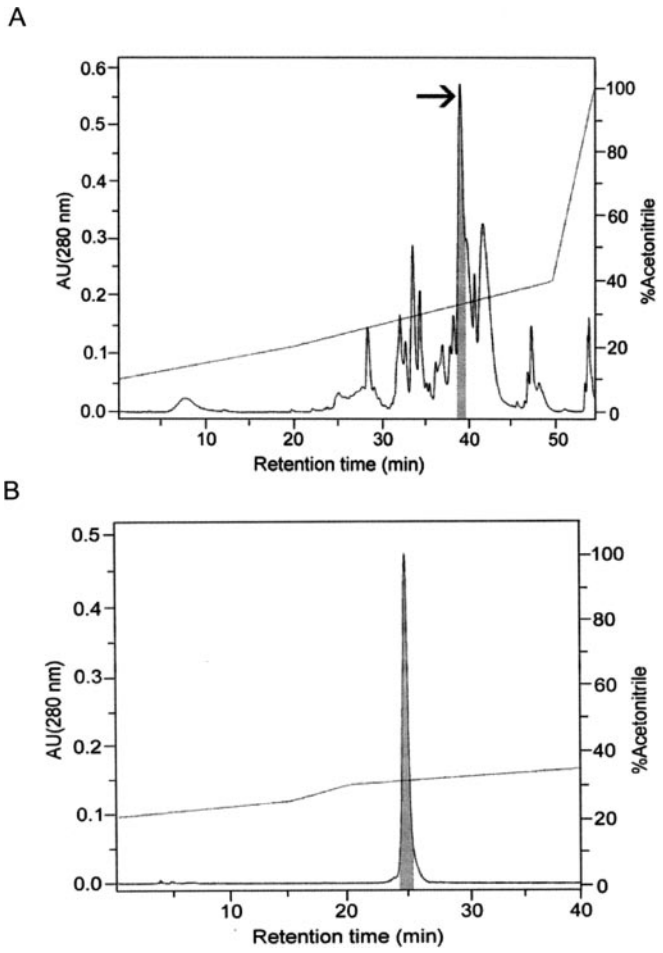

FIG. 1. **Purification of JZTX-III.** *A*, an RP-HPLC chromatogram of crude *C. jingzhao* venom. The wanted peak is indicated with an *arrow*. *AU*, arbitrary units. *B*, further purification of JZTX-III by a repetitive RP-HPLC. In both *A* and *B*, the collected peak areas are *shaded* in *gray*. The linear gradient of buffer B (acetonitrile) is indicated with a *dashed line*.

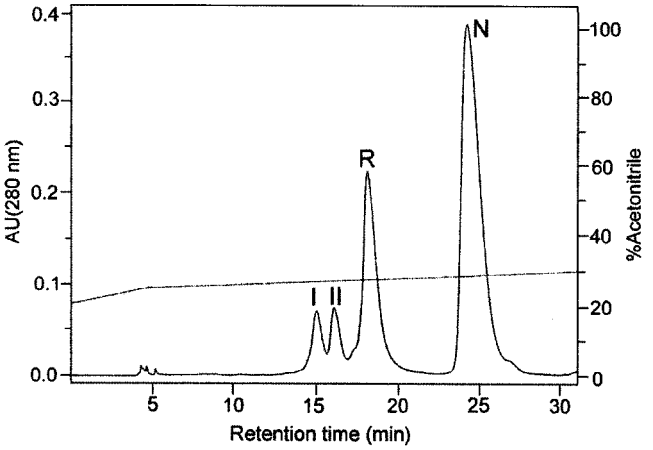

FIG. 2. **Analytical RP-HPLC chromatogram of partial reduced JZTX-III by TCEP.** Four chromatographic peaks contained intact peptide and partially reduced intermediates, respectively. As determined by MALDI-TOF mass spectrometry, their molecular masses had 2 (*peak I*), 4 (*peak II*), 6 (*peak R*), or 0 Da (*peak N*) more than that of native JZTX-III, respectively, suggesting that the main peak (*peak N*) represented intact toxin and that *peak R* represented completely reduced peptide, whereas two intermediates contained only one (*peak II*) or two (*peak I*) disulfide bonds.

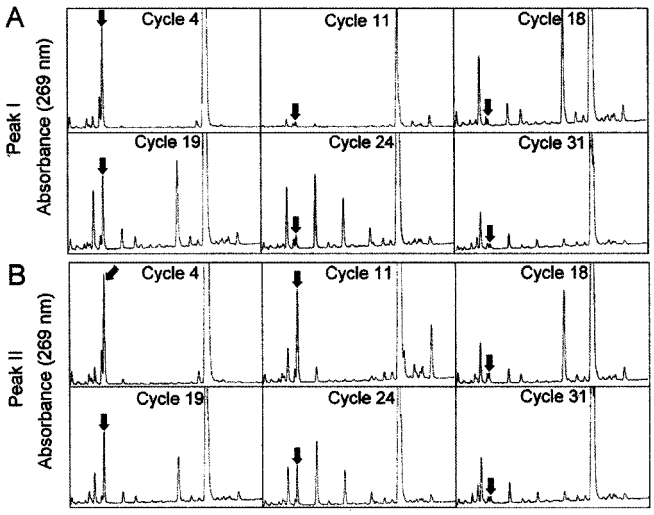

FIG. 3. **RP-HPLC profile of sequencing partially reduced intermediates modified with iodoacetamide.** Cys residues occur at cycles 2, 9, 16, 17, 22, and 29. The elution position of Pth-CM-Cys is marked with *down arrows*. *A*, the Cys residue cycles of alkylated peak I in Fig. 2. *B*, the Cys residue cycles of alkylated peak II in Fig. 2.

I, whereas no signals emerged at other cysteine cycles. The result indicates that the only reduced disulfide bond is Cys^4–Cys^{19}. When sequencing alkylated peak II, Pth-CM-Cys signals were observed at the 4th, 11th, 19th, and 24th cycles in the profiles of cysteine cycles (Fig. 3*B*), indicating that Cys^{18} was still linked to Cys^{31} by a disulfide bond. The above results indicate that two of three disulfide bridges in JZTX-III were determined to be Cys^4–Cys^{19} and Cys^{18}–Cys^{31}. Accordingly, the third one is cross-linked between Cys^{11} and Cys^{24}. Thus, JZTX-III has a conserved disulfide connectivity emerging among ICK motifs where 6 cysteines were linked in a pattern of I-IV, II-V, and III-VI (9).

Cloning and Sequencing of JZTX-III cDNA—The full-length cDNA sequence of JZTX-III was completed by overlapping two fragments resulting from 3′- and 5′-RACE. As shown in Fig. 4*B*, the oligonucleotide sequence of the cDNA was a 373-bp bond in which the first ATG was assumed to serve as the translation start codon. The open reading frame, ending before the first stop codon TGA at 3′-terminal position, encoded 63 residues corresponding to the JZTX-III precursor. It comprised a signal peptide of 21 residues, a pro-peptide of 5 residues, and a mature peptide of 36 residues. The deduced mature peptide sequence was consistent with that of native JZTX-III determined by Edman degradation. Unlike huwentoxin-IV, JZTX-III had no extra Gly or Gly + Arg/Lys residues at the C terminus, which are known to allow "post-modification" α-amidation at the C-terminal residue (20). The prepro-regions common to all spider toxins are a hydrophobic peptide and can be processed at a common signal site -*X*-Arg- before mature peptide sequences, which is recognized by special endoprotelytic enzymes. In general, this region is composed of over 40 residues. Interestingly, further analysis indicated that JZTX-III had a very small prepro-region that exhibits no similarity to those of other spider toxins from diverse species including the Chinese bird spider *Selenocosmia huwena* Wang (also known as *Ornithoctonas huwena* Wang) (20, 21). Furthermore, it is worth noting that the signal site anterior to mature JZTX-III was an uncommon one (-*X*-Ser-) (20, 23–25). A polyadenylation signal, AATAAA, was found in the 3′-untranslated region at position 16 upstream of the poly(A).

Effects of JZTX-III on VGSCs—Using whole cell patch clamp technique, the actions of JZTX-III were characterized on VGSCs in rat DRG neurons and ventricular myocytes, in which both TTX-S and TTX-R types are co-expressed. TTX (200 nM) was added to the external bath solution to separate TTX-R type

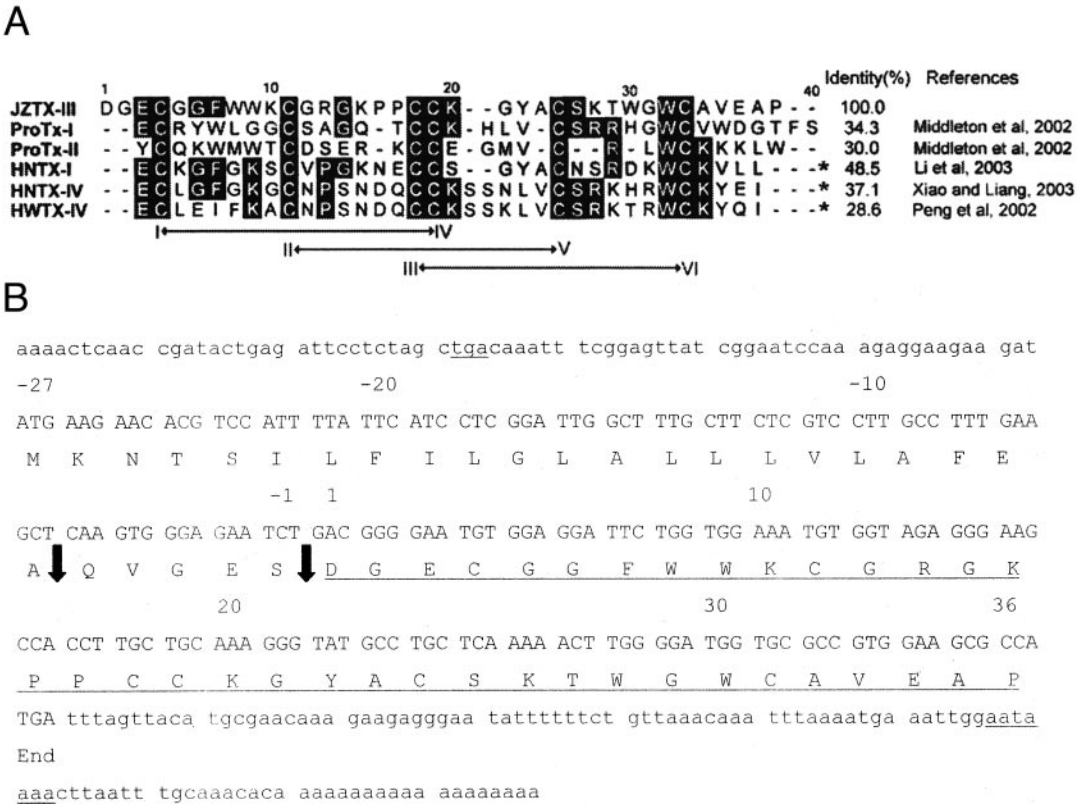

FIG. 4. **Amino acid sequence (*A*) and cDNA sequence (*B*) of JZTX-III.** *A*, comparison of the primary structures of six sodium channel toxins: JZTX-III, ProTx-I, ProTx-II, HNTX-I, HNTX-IV, and HWTX-IV. Except for JZTX-III and ProTxs, others had an amidated C terminus. ProTx-I and ProTx-II were isolated from the venom of the tarantula *Thrixopelma pruriens*. HNTX-I, HNTX-IV, and HWTX-IV were isolated from the venoms of the Chinese bird spiders *Selenocosmia hainana* and *S. huwena*, respectively. The identical residues are *shaded* in *black*. The disulfide bridge pattern of the toxins is indicated *under* their sequences. JZTX-III inhibited activation of TTX-R VGSCs in rat cardiac myocytes. ProTx I–II inhibited the activation of $Na_v1.2$, 1.5, 1.7, and 1.8 expressed in human embryonic kidney (HEK) cells. HNTX-I blocked $rNa_v1.2$ and para/tipE expressed in *Xenopus laevis* oocytes. Both HWTX-IV and HNTX-IV blocked TTX-S VGSCs in DRG neurons. *B*, the cDNA sequence of JZTX-III. The precursor deduced from the cDNA is indicated *below* the nucleotide acid sequence. The amino acid sequence of mature toxin is *underlined*. The possible endoprotelytic sites are pointed out with *down arrows*. An *asterisk* indicates that the C-terminal carboxyl group is amidated.

from mixture currents. Although Maier *et al.* (26) suggested that some brain TTX-S subtypes were situated in transverse tubules of ventricular myocytes, in our experiments, the induced sodium currents were not changed in the absence or presence of TTX at 0.2 μM (data not shown, $n = 4$). Therefore, the effects of JZTX-III on cardiac myocytes were assayed in bath solution without TTX.

After establishing whole cell configuration, the experimental cells were held at −80 mV for over 4 min to allow adequate equilibration between the micropipette solution and the cell interior, and then the current traces were evoked using a 50-ms step depolarization to −10 mV every second. As shown in Fig. 5, *A* and *B*, 1 μM JZTX-III showed no evident effects on the normal activities of both TTX-S and TTX-R VGSCs in DRG neurons ($n = 3$). However, cardiac TTX-R currents were sensitive to the novel toxin. 1 μM JZTX-III reduced the control peak amplitude to a maximum effect by 64.7 ± 4.7% (Fig. 5*C*, $n = 8$). JZTX-III up to 10 μM completely eliminated the remaining currents within less than 1 min (Fig. 5, *D* and *E*, $n = 4$). The rapid inhibition was dose-dependent with an IC_{50} value of 0.38 ± 0.04 μM (Fig. 5*F*). It was observed that similar to ProTx I–II (15), JZTX-III failed to alternate channel inactivation, although most spider toxins (*e.g.* δ- and μ-toxins) identified to date share a common mode of slowing channel inactivation similar to scorpion α-toxins (7). ProTx I–II have been suggested to bind to VGSC site 3 or site 4. To further determine the detailed site for the toxin of interest, a simple competitive assay was introduced between JZTX-III and site 3 toxins. *Buthus martensi* Karsch I (BMK-I), acting on site 3, is a typical α-like scorpion toxin isolated from the Asian scorpion, *B. martensi* Karsch. It can slow the inactivation of VGSCs expressing in both mammalian sensory neurons and ventricular myocytes without significantly affecting the peak amplitudes (10, 27). Exposed to 10 μM JZTX-III, the slowing currents induced by 10 μM BMK-I were eliminated completely, suggesting that the spider toxin modulated cardiac VGSCs through a mechanism distinct from site 3 toxins.

Fig. 6 shows the current-voltage (I-V) curve of cardiac TTX-R VGSCs, yielding that initial activated voltage and reversal potential are −50 mV and +25 mV, respectively ($n = 4$). After 1 μM JZTX-III treatment for 1 min, the inhibition of currents could be observed at tested potential from −40 mV to +20 mV. JZTX-III shifted the threshold of initial activation more than +10 mV in a depolarizing direction, but no change was observed significantly in the membrane reversal potential, implying that it did not change the ion selectivity of channels.

Effects of JZTX-III on VGCCs and Voltage-gated Potassium Channels (VGPCs)—There are two main categories of VGCCs distributed in rat DRG neurons: high voltage-activated channels and low voltage-activated channels, which can be discriminated by their voltage dependence and kinetics. JZTX-III (1 μM) was not found to affect VGCCs (Fig. 7, $n = 3$). Three different VGPC isoforms ($K_v1.1$, $K_v1.2$, and $K_v1.3$) were expressed in *Xenopus Laevis* oocytes and checked for toxins using the two-electrode voltage clamp technique as described previously (28). No effects were detected with JZTX-III at 1 μM (Fig. 8, $n = 4$).

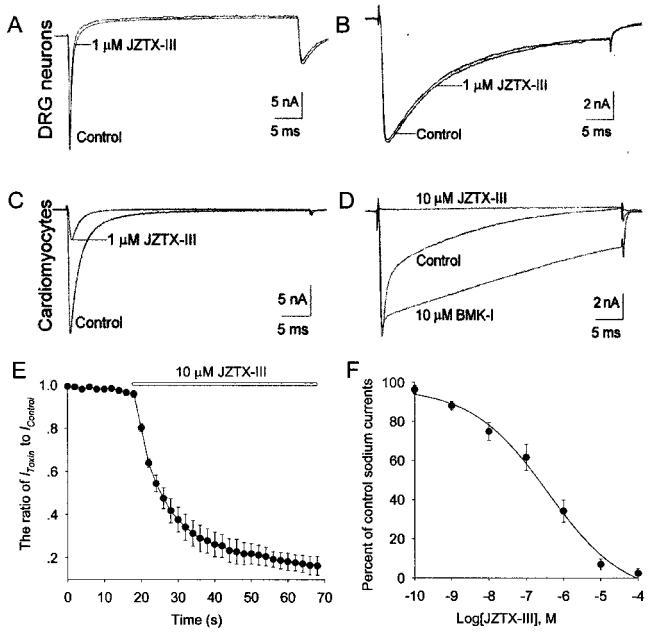

FIG. 5. **Effects of JZTX-III on VGSCs.** All current traces were evoked by a 50-ms step depolarization to −10 mV from a holding potential of −80 mV at every 2 s. Both TTX-S (*A*) and TTX-R (*B*) VGSCs were significantly unaffected by 1 μM HNTX-I on DRG neurons, isolated from adult rat by the method described in Ref. 18. *C*, effects of TTX-R sodium currents in cardiac myocytes. 1 μM JZTX-III evidently reduced the control current amplitude by 64.7 ± 4.7% ($n = 8$), whereas at 10 μM, the toxin eliminated the slowing inward current induced by 1 μM BMK-I (*D*, $n = 4$) in a time-dependent manner (*E*, $n = 4$). *F*, the concentration-dependent inhibition of TTX-R sodium currents in cardiac myocytes. Every data point (mean ± S.E.) coming from 3–8 cells shows current relative to control. These data points were fitted according to Boltzmann equation (see "Materials and Methods").

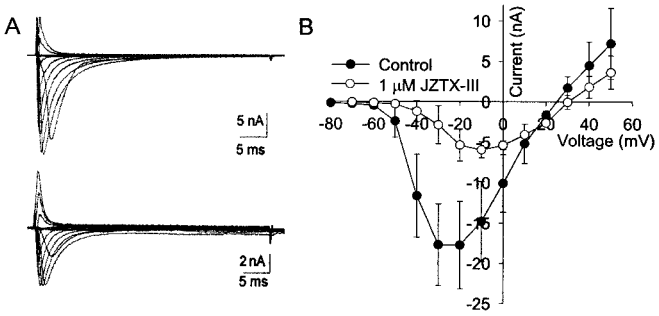

FIG. 6. **Effects of JZTX-III on the current-voltage (I-V) relationship of TTX-R VGSCs in cardiomyocytes.** A family of currents was elicited by 50-ms depolarizing steps to various potentials from a holding potential of −80 mV. Test potentials ranged from −80 mV to +50 mV at increments of +10 mV. The I-V curve (*B*) of sodium currents showed the relationship between current traces before (*above*) and after (*below*) adding 1 μM JZTX-III in *A*. In *B*, the data points obtained from four separated experimental cells are shown as mean ± S.E.

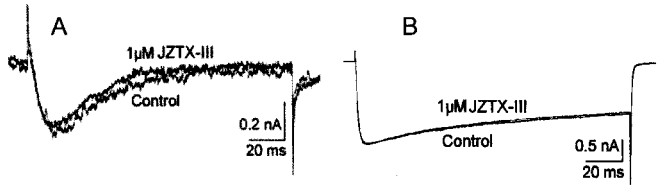

FIG. 7. **Effects of JZTX-III on VGCCs on rat DRG neurons.** *A*, high voltage-activated currents were elicited by a 150-ms depolarizing voltage of 0 mV from a holding potential of −40 mV, and current traces were not changed before and after the application of 1 μM JZTX-III. *B*, low voltage-activated currents were induced by a 150-ms depolarizing potential of −30 mV from a holding potential −90 mV, and current traces were not changed before and after the application of 1 μM JZTX-III.

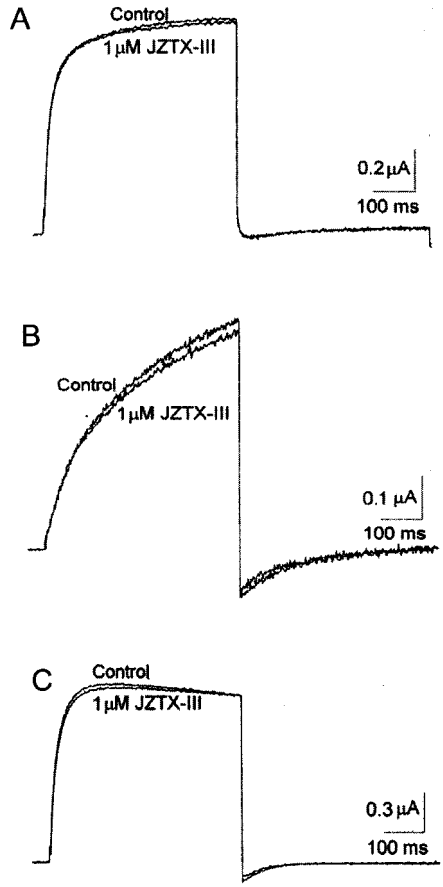

FIG. 8. **Effects of JZTX-III on VGPCs expressed in *X. laevis* oocytes.** $K_v1.1$ (*A*), $K_v1.2$ (*B*), and $K_v1.3$ (*C*) current traces were evoked by depolarizations to +10 mV from a holding potential of −90 mV. After exposure to 1 μM JZTX-III, no changes of the currents were detected.

DISCUSSION

In this work, we have isolated and characterized a 3.9-kDa toxin named JZTX-III from the Chinese spider *C. jingzhao* (19). The full sequence of the toxin was performed by Edman degradation and found to contain 36 residues including 6 cysteines. No amidation at its C-terminal residue is detected by MALDI-TOF mass spectrometry and its cDNA sequence analysis. Although it exhibits less than 50% sequence identity to any known peptides, it contains a conserved disulfide connectivity frequently emerging in ICK peptide toxins from diverse species, such as spiders and marine snails, cross-linked in a pattern of I–IV, II-V, and III-VI. Based on the analysis of precursor organization and gene structure combined with a three-dimensional fold, Zhu *et al.* (29) suggested that these ICK peptides from animals shared a common evolutionary origin. The molecular scaffold is highly stabilized by the three disulfide bridges, especially the third (III-VI) (9). Huwentoxin-II, from the Chinese bird spider *S. huwena*, adopts a scaffold distinct from ICK motif for having a unique disulfide connectivity of I-V, II-III, and IV-VI (30). The residue numbers between 2 cysteines in JZTX-III also conform exactly to the ICK definition described as a consensus sequence $C_IX_{3-7}C_{II}X_{4-6}C_{III}C_{IV}X_{1-4}C_VX_{4-13}C_{VI}$ (where *X* is any residue, with the number indicated by the range) (9).

The amino acid sequence of JZTX-III is verified further by its cDNA, which produces a precursor comprising a signal peptide, an intervening pro-peptide, and a mature peptide. Concerning the structural organization, JZTX-III should be matured through a post-translational cleavage during the course of se-

cretion. Many works have demonstrated that there is a common endoprotelytic site (-*X*-Arg-) between the sequences of prepro and mature peptide (20, 23–25). Different from known spider toxins, JZTX-III precursor contains an uncommon site (-*X*-Ser-), suggesting that the processing to endroproteolysis prepro-peptide should be accordingly different from that of them. Another intriguing finding in this study is that the intervening pro-peptide region of JZTX-III is the smallest one identified to date in the field of spider toxins. The region, generally rich in glutamate residues, emerges in cDNA sequences of most animal toxins from diverse sources, but it is missing in some scorpion toxins. Until now, its action in forming toxins is not yet well defined, although Diao *et al.* (20) inferred that it might contribute to stabilizing the toxin precursor and prevent the mature toxins from interacting with other molecules in the cytoplasm. Furthermore, the analysis of prepro-regions can provide new proof for interpreting the evolutionary relationship in animal toxins. Around 50,000 conotoxins, although targeting different receptors, can be grouped into seven superfamilies (24). However, no similar description about spider toxins demonstrated that their prepro-peptides share higher sequence identity with one another, until in our recent work, seven distinct cDNAs from the gland of *S. huwena* were classified into two superfamilies (20). Having two distinct characterizations, an uncommon endoproteolytic site (-*X*-Arg-) and a very small pre-region exhibiting limited sequence identity to others, JZTX-III defines a novel superfamily distinct from the previously reported two superfamilies.

To date, more than 30 spider toxins from BLAST databases are found to target neuronal VGSCs, but few are found to target the cardiac subtype. According to their distinct pharmacological characterization, these toxins can be classified into two groups: excitatory toxins and depressant toxins (21). ProTx-I and ProTx-II are the only agents reported in the both groups to inhibit $Na_v1.5$, a TTX-R subtype expressing especially in cardiac myocytes (17). A similar inhibition of channel activation is observed after the application of JZTX-III, and it belongs to the depressant toxins. It seems that its selectivity for sodium channel isoforms is even higher than that of ProTxs, which inhibit some neuronal VGSC subtypes ($Na_v1.2$, $Na_v1.8$–1.9) with IC_{50} values of less than 0.1 μM. Moreover, ProTxs target outward delayed-rectifier VGPCs and T-type VGCCs (17). We also checked the effects of JZTX-III on neuronal VGSCs isoforms and VGCCs as well as VGPCs ($K_v1.1$–1.3) expressed in *Xenopus laevis* oocytes, but no evident effects were observed. It is very likely that $Na_v1.4$ is not the target for JZTX-III because the peptide did not affect the normal contractions of mouse diaphragm induced by direct electrical stimulus. The properties of JZTX-III in $Na_v1.5$ are similar to those of scorpion β-toxins. They inhibit channel activation without affecting the inactivation kinetics or the ion selectivity of Na^+ (10). This mechanism is different from that of excitatory spider toxins, such as δ-actracotoxin-Ar1, in which they, binding to the extracellular S3-S4 loop of domain IV, modify the conformation of channel peptides and cause an uncoupling of channel activation and inactivation in a similar manner to scorpion α-toxins or sea anemone toxins (14). In our experiments, JZTX-III inhibited the slowing currents induced by site 3 toxin (BMK-I, a scorpion α-like toxin) completely, suggesting that the binding site for the spider toxin is not site 3. The mechanism of JZTX-III is also different from that of other depressant toxins, such as HNTX-IV. They block neuronal TTX-S VGSCs with no shift in the I-V curve and are assumed to be site 1-like toxins (16, 18). According to the distinct effects on the VGSCs when toxins selectively bind to six sites of the channels (12), JZTX-III can be reasonably inferred to interact with site 4 located at the extracellular S3-S4 loop of domain II of the channel molecules. Furthermore, it is worth noting that although both β-scorpion toxin and JZTX-III inhibit channel activation, they cause a shift of the voltage dependence in different directions, implying that these toxins do not overlap the same active residues at site 4 of the VGSC protein. Thus, JZTX-III hopefully represents a useful probe for discriminating rat cardiac TTX-R VGSC isoform, although it has a lower affinity ($IC_{50} < 0.4$ μM).

Naturally occurring toxin determinants are helpful for insight into the underlying mechanism of peptides responding to distinct receptors. NMR structures of hainantoxin-I (HNTX-I) and ProTxs reveal that a hydrophobic patch formed by Phe, Tyr, Trp, and Val act as an ion channel binding site anchor and charged residues can be responsible for their pharmacological specificity (17, 21). Sequence alignment in Fig. 4*A* indicates that JZTX-III shows limited sequence identities with other sodium channel toxins (*e.g.* HNTX-I and ProTxs). However, interestingly, several hydrophobic residues (Phe^7, Tyr^{22}, Trp^{30}, and Val^{33}) in JZTX-III are strictly conserved at the corresponding positions in other sodium channel toxins. HNTX-IV is a potent blocker of neuronal TTX-S VGSC in DRG neurons with an IC_{50} value of 44.6 nM (18). Substitutions of Lys^{27} or Arg^{29} with Ala reduce HNTX-IV sensitivity of TTX-S VGSC in DRG neurons by over 10-fold.[2] The 2 positive residues are also conserved in HWTX-IV, ProTxs, and HNTX-I, which are proved to inhibit $Na_v1.2$, whereas they are missing in JZTX-III. It is likely that the 2 residues may be responsible for binding $Na_v1.2$ but not $Na_v1.5$. JZTX-III has 8 charged residues, and most of them, except for Asp^1 and Arg^{13}, can be found at corresponding positions in neurotoxins. From the listed sequences, it is still difficult to infer the crucial residues responsible for Nav1.5, but we can assume that Asp^1 and Arg^{14} may result in the subtle difference in pharmacological characterization between JZTX-III and other toxins.

Acknowledgments—We gratefully acknowledge Dr. Jan Tytgat at Leuven University for checking jingzhaotoxin-III on the $K_v1.1$, $K_v1.2$, and $K_v1.3$ expressed in *Xenopus laevis* oocytes. We thank Prof. Yonghua Ji at Shanghai Life Sciences Institute for presenting BMK-I.

REFERENCES

1. Sokolova, O., Kolmakova-Partensky L., and Grigorieff, N. (2001) *Structure* **9,** 215–220
2. Sato, C., Ueno, Y., Asai, K., Takahashi, K., Sato, M., Engel, A., and Fujiyoshi, Y. (2001) *Nature* **409,** 1047–1051
3. Lopreato, G. F., Lu, Y., Southwell, A., Athinson, N. S., Hillis, D. M., Wilcox, T. P., and Zakon, H. (2001) *Proc. Natl. Acad. Sci. U. S. A.* **98,** 7588–7592
4. Ogata, N., and Ohishi, Y. (2002) *Jpn. J. Pharmacol.* **88,** 365–377
5. Goldin, A. L., Barchi, R. L., Caldwell, J. H., Hofmann, F., Howe, J. R., Hunter, J. C., Kallen, R. G., Mandel, G., Meisler, M. H., and Berwald, N. (2000) *Neuron* **28,** 365–368
6. Goldin, A. L. (2002) *J. Exp. Biol.* **205,** 575–584
7. Cummins, T. R., Aglieco, F., Renganathan, M., Herzog, R. I., Dib-Hajj, S. D., and Waxman, S. G. (2001) *J. Neurosci.* **21,** 5952–5961
8. Herzog, R. I., Liu, C. J., Waxman, S. G., and Cummins, T. R. (2003) *J. Neurosci.* **23,** 8261–8270
9. Escoubas, P., Diochot, S., and Corzo, G. (2000) *Biochimie* (*Paris*) **82,** 893–907
10. Goudeta, C., Chi, C. W., and Tytgata, J. (2002) *Toxicon* **40,** 1239–1258
11. Sun, Y. M., Bosmans, F., Zhu, R. H., Goudet, C., Xiong, Y. M., Tytgat, J., and Wang, D. C. (2003) *J. Biol. Chem.* **278,** 24125–24131
12. Cestele, S., Ben Khalifa, R. B., Pelhate, M., Rochat, H., and Gordon, D. (1995) *J. Biol. Chem.* **270,** 15153–15161
13. Omecinsky, D. O., Holub, K. E., Adams, M. E., and Reily, M. D. (1996) *Biochemistry* **35,** 2836–2844
14. Nicholson, G. M., Walsh, R., Little, M. J., and Tyler, M. I. (1998) *Pfluegers Arch. Eur. J. Physiol.* **436,** 117–126
15. Corzo, G., Gilles, N., Satake, H., Villegas, E., Dai, L., Nakajima, T., and Haupt, J. (2003) *FEBS Lett.* **547,** 43–50
16. Peng, K., Shu, Q., Liu, Z., and Liang, S. (2002) *J. Biol. Chem.* **49,** 47564–47571
17. Middleton, R. E., Warren, V. A., Kraus, R. L., Hwang, J. C., Liu, C. J., Dai, G., Brochu, R. M., Kohler, M. G., Gao, Y. D., Garsky, V. M., Bogusky, M. J.,

[2] D. Li, Y. Xiao, X. Xu, X. Xiong, M. Wang, Z. Lin, X. Gu, and S. Liang, unpublished work.

Mehl, J. T., Cohen, C. J., and Smith, M. M. (2002) *Biochemistry* **41,** 14734–14747
18. Xiao, Y. C., and Liang, S. P. (2003) *Eur. J. Pharmacol.* **477,** 1–7
19. Zhu, M. S., Song, D. X., and Li, T. H. (2001) *J. Baoding Teachers Coll.* **14,** 1–6
20. Diao, J. B., Lin, Y., Tang, J. Z., and Liang, S. P. (2003) *Toxicon* **42,** 715–723
21. Li, D. L., Xiao, Y. C., Hu, W. J., Xie, J. Y., Bosmans, F., Tytgat, J., and Liang, S. P. (2003) *FEBS Lett.* **555,** 616–622
22. Cao, C. M., Xia, Q., Chen, Y. Y., Zhang, X., and Shen, Y. L. (2002) *Pfluegers Arch. Eur. J. Physiol.* **443,** 635–642
23. Cardoso, F. C., Pacifico, L. G., Carvalho, D. C., Victoria, J. M., Neves, A. L., Chavez-Olortegui, C., Gomez, M. V., and Kalapothakis, E. (2003) *Toxicon* **41,** 755–763
24. Wang, C. Z., Jiang, H., Ou, Z. L., Chen, J. S., and Chi, C. W. (2003) *Toxicon* **42,** 613–619
25. Alami, M., Vacher, H., Bosmans, F., Devaux, C., Rosso, J. P., Bougis, P. E., Tytgat, J., Darbon, H., and Martin-Eauclaire, M. F. (2003) *Biochem. J.* **375,** 551–560
26. Maier, S. K., Westenbroek, R. E., Schenkman, K. A., Feigl, E. O., Scheuer, T., and Catterall, W. A. (2002) *Proc. Natl. Acad. Sci. U. S. A.* **99,** 4073–4078
27. Ji, Y. H., Mansuelle, P., Terakawa, S., Kopeyan, C., Yanaihara, N., Hsu, K., and Rochat, H. (1996) *Toxicon* **34,** 987–1001
28. Huys, I., and Tytgat, J. (2003) *Eur. J. Neurosci.* **17,** 1786–1792
29. Zhu, S., Darbon, H., Dyason, K., Verdonck, F., and Tytgat, J., (2003) *FASEB J.* **17,** 1765–1767
30. Shu, Q., Lu, S. Y., Gu, X. C., and Liang, S. P. (2002) *Protein Sci.* **11,** 245–252